

---

EFDA–JET–CP(03)04-04

M.J. Rubel, J.P. Coad, P. Wienhold, G. Matthews, V. Philipps,  
M. Stamp and T. Tanabe

# Fuel Inventory and Co-Deposition in Grooves and Gaps of Divertor and Limiter Structures



# Fuel Inventory and Co-Deposition in Grooves and Gaps of Divertor and Limiter Structures

M.J. Rubel<sup>1</sup>, J.P. Coad<sup>2</sup>, P. Wienhold<sup>3</sup>, G. Matthews<sup>2</sup>, V. Philipps<sup>3</sup>, M. Stamp<sup>2</sup>,  
T. Tanabe<sup>4</sup> and JET EFDA Contributors\*

<sup>1</sup>*Alfvén Laboratory, Royal Institute of Technology (KTH), Association EURATOM-VR, 100 44  
Stockholm, Sweden*

<sup>2</sup>*EURATOM/UKAEA Fusion Association, Culham Science Centre, Abingdon, OX14 3DB, UK*

<sup>3</sup>*Institute of Plasma Physics, Forschungszentrum Jülich, Association EURATOM, D-52425  
Jülich, Germany*

<sup>4</sup>*Centre for Integrated Research in Science and Engineering (CIRSE), Nagoya University,  
Chikusa-ku, 464 Nagoya, Japan*

\* See annex of J. Pamela et al, "Overview of Recent JET Results and Future Perspectives",  
*Fusion Energy 2000 (Proc. 18<sup>th</sup> Int. Conf. Sorrento, 2000), IAEA, Vienna (2001).*

Preprint of Paper to be submitted for publication in Proceedings of the  
10th International Workshop on Carbon Materials for Fusion Application  
(Jülich, Germany, 17-19 September 2003)

“This document is intended for publication in the open literature. It is made available on the understanding that it may not be further circulated and extracts or references may not be published prior to publication of the original when applicable, or without the consent of the Publications Officer, EFDA, Culham Science Centre, Abingdon, Oxon, OX14 3DB, UK.”

“Enquiries about Copyright and reproduction should be addressed to the Publications Officer, EFDA, Culham Science Centre, Abingdon, Oxon, OX14 3DB, UK.”

## **ABSTRACT.**

Plasma facing components from JET and TEXTOR were studied. The emphasis was on the comparison of co-deposition, material mixing and fuel inventory on plasma facing and side surfaces of tiles, i.e. in gaps separating the tiles. Integrated fuel content in gaps of the Mk-I JET divertor floor was approximately two times greater than detected on the plasma facing surfaces. Taking into account similarities between the Mk-I structure and the castellation in the ITER divertor, the impact of the tile shaping on the tritium inventory is addressed. Deposition on the side of limiter tiles in TEXTOR was around 20% of that on the plasma facing surfaces. Experiments aiming at a deeper insight into the deposition on ITER-relevant components are also proposed.

## **1. INTRODUCTION**

Castellated structure of tiles in the ITER divertor is deemed as the best solution to ensure thermo-mechanical durability and integrity of materials under high heat flux loads, especially when the use of tungsten is considered [1-4]. It is known, however, that in the environment containing also low-Z elements (e.g. carbon), eroded material is transported and co-deposited together with fuel species in areas shadowed from the direct plasma line-of-sight [5-10]. In a consequence, re-deposition and material mixing may occur in grooves and on side surfaces of plasma facing components (PFC), e.g. on surfaces located in gaps separating the tiles. Such deposition has been observed, but quantitative results have not been published before. The issue is quite important because in the gaps significant amount of fuel may become accumulated. Based on the experience from JET, co-deposits formed in remote areas (e.g. inner divertor corner and water-cooled louvers) are very difficult to remove by cleaning methods [11] and this results in significant long-term fuel retention [9,12,13]. Similarly, on a reasonable time scale, it may be difficult to remove fuel from the castellation by means of known [11] and proposed cleaning techniques [14-16]. It should be noted that the surface area in gaps of the ITER divertor will be approximately three times bigger than the area of plasma facing surfaces. Secondly, very limited access to in-vessel components of ITER calls for a more detailed studies of deposition in gaps and grooves of PFC from present-day devices. The intention of this work is to bring an overview of results gathered over years at the JET and TEXTOR tokamaks and to give an approximate assessment of the fuel inventory and material mixing occurring on side surfaces of divertor, limiter and diagnostic components.

## **2. EXPERIMENTAL**

A number of PFC and various probes were examined ex-situ after long-term plasma operation periods. From JET these were carbon fibre composite (CFC) tiles and Langmuir probes from a poloidal cross-section of the Mk-I divertor. Limited research has been also carried out for side surfaces of tiles from the Mk-IIA and Mk-IIGB (Gas Box) divertors. There were several reasons for revisiting the Mk-I divertor operated in 1994-1995 first with Carbon Fibre Composite (CFC) and then with beryllium tiles: the resemblance of tile positioning to the castellation and the fact, that it

was the largest structure of this kind ever used in fusion experiments. Moreover, beryllium tiles were castellated. It was also considered worthwhile to repeat the deuterium analysis several years after the first examination in order to check whether the D content has significantly changed over that period of time. Figure 1(a) shows the JET vessel with the Mk-I divertor. A schematic drawing in Fig.1(b) shows the shape and positioning of tiles and probes with respect to the field lines. These tiles were 72mm long poloidally and from 30 (inner divertor) up to 40mm (outer) wide toroidally. Castellation in the Be tiles was  $6 \times 6$ mm with a  $\sim 0.6$ mm wide and 10mm deep groove. The probes were  $64\text{mm}^2$  in horizontal cross-section ( $8\text{mm} \times 8\text{mm}$ ) and 48 mm long. The gap separating tiles was 2 to 6mm wide toroidally and 6 or 10mm poloidally. Due to the trapezoid and roof-like shaping, the upper edge of one poloidally-oriented tile was shadowing the gap and a part of the adjacent one. On the other hand, the toroidally-oriented side surfaces in gaps were not shadowed. More details regarding the divertor structure can be found elsewhere [5,6]. The pump was located behind the outer divertor wing and pumping was realised through gaps between tiles. The divertor was water-cooled and the base temperature of tiles was in the  $30\text{-}50^\circ\text{C}$  range. The total plasma operation time was 59661s and 20303s including 25594s and 9153s of the X-point plasma for the CFC and Be divertors, respectively. The strike points were located on the floor tiles only.

Two other divertors (IIA and IIGB) were constructed with much larger tiles with plasma facing surface of up to  $500\text{cm}^2$ . Therefore, the surface area of side surfaces and the projected area of gaps between the tiles were significantly smaller than in the Mk-I structure. Pumping channels were in the divertor corners only. Another major difference was the base temperature of MK-IIA and GB maintained in the range from  $250$  to  $300^\circ\text{C}$ .

In case of TEXTOR, the investigation was carried out for various graphite and composite limiters. Toroidal belt pumped limiter ALT II is the main PFC of TEXTOR. Pumping is realised through the channels located beneath the limiter support structure. Graphite tiles (side and rear surfaces) of the toroidal belt limiter ALT II were examined regularly after campaigns lasting 14000 – 15000 plasma operation seconds. The tiles were approximately 100mm wide, 150mm long and from 10 to 14mm thick and separated by a 4mm wide gaps. Details regarding the belt limiter can be found in [17-19]. Tungsten-coated graphite blocks of the main poloidal limiter (after 750 plasma-seconds) were mounted in arrays of five and the gap between the tiles was 6mm wide at the plasma radius [10,20]. In graphite-tungsten twin limiters [8] the gap width was 5mm. The base temperature of all graphite components was in the range  $300\text{-}350^\circ\text{C}$ , whereas the solid tungsten block of the twin limiter was maintained at above  $450^\circ\text{C}$  in order to avoid its cracking caused by thermal shocks.

Nuclear reaction analysis (NRA) was used for the quantification of deuterium [ $d(^3\text{He,p})\alpha$ ], carbon [ $^{12}\text{C}(^3\text{He,p})^{14}\text{N}$ ], beryllium [ $^9\text{Be}(^3\text{He,p})^{11}\text{B}$ ] and boron [ $^{11}\text{B}(p,\alpha)^8\text{Be}$ ]. Most of D, Be and C analyses was carried out with a  $2.5\text{MeV } ^3\text{He}^+$  beam, but to assess the thickness of deuterium-containing deposits, the  $^3\text{He}$  beam energy was occasionally scanned in the range  $0.7 - 3\text{MeV}$  giving the information depth from 1.3 to approximately 10 microns, respectively. Rutherford Backscattering Spectroscopy (RBS) was applied for determining the content of tungsten and other medium and

high-Z elements, whereas Enhanced Proton Scattering (EPS) was used for analysis of carbon [ $^{12}\text{C}(\text{p,p})^{12}\text{C}$ ] on tungsten.

### 3. RESULTS AND DISCUSSION

#### 3.1 JET

Images in Fig.2(a) and (b) show the general appearance of the Mk-I divertor after the operation with CFC and beryllium tiles, respectively. Deposits are seen predominantly at the inner and outer sections and even on the supporting rails, whereas tiles in the central part are fairly shine with little deposition. From Fig.3 one infers that the deposition in gaps differs on the two sides: distinct deposition on the shaded surface and fairly little on the shadowing one. Details presented in Fig. 4 for plasma facing and side surfaces of CFC tiles and Langmuir probes from the Mk-I divertor prove the presence of flaking films. On toroidally-oriented side the film is found to the end of tiles, i.e. 50mm deep towards the bottom of the divertor. Moreover, inspecting the probes one directly perceives the effects of erosion and deposition resulting from the roof-like tile shaping. While the tip of the probe on the left side of Fig.4(b) is flat and with sharp edges, the other probe has somewhat rounded upper edge due to erosion and a macro deposit ( $\sim 0.15\text{mm}$  thick) is seen near the lower edge which was shaded by the adjacent tile.

The composition of plasma facing surfaces of the divertor floor was reported after the analysis of twenty tiles, i.e. one whole poloidal set composed of two rows with ten tiles each ( $0.0504\text{m}^2$ , projected area of gaps subtracted) [5,6]. Deuterium content measured in the inner divertor was somewhat greater than in the outer section. On many tiles the maximum inventory was detected in narrow deposition belts (over  $5 \times 10^{19}$  D at  $\text{cm}^{-2}$ , approximately 5mm wide) in the shadowed part. Secondly, there were no areas with the concentration lower than  $5 \times 10^{17}$  D at  $\text{cm}^{-2}$  and this level could be associated with the deuterium directly implanted to the saturation level during the plasma impact. Taking into account the results of detailed mapping of the deuterium distribution on the analysed tiles [5] and assuming toroidal symmetry of the deposition pattern one assesses the total inventory on the entire area of plasma facing surfaces on the divertor floor ( $11.1\text{m}^2$ , projected area of gaps subtracted) on the level of  $8.86 \times 10^{23}$  D at  $\text{cm}^{-2}$ . This value should be treated as a lower limit, because the information depth for deuterium with NRA using a  $2.5\text{MeV } ^3\text{He}^+$  beam is limited to approximately 8 – 8.5 microns, whereas thicker co-deposits with very high deuterium content ( $> 5 \times 10^{19} \text{cm}^{-2}$ ) and high concentration ratio of deuterium-to-carbon,  $\text{D}/\text{C} > 0.5$ , were detected on some tiles. The presence of such regions was confirmed by scanning the energy of the analysing beam up to 3MeV and detecting a still increasing proton signal associated with deuterium in the layer at least 10 – 10.5 microns thick. Figure 5 shows the deuterium (a) and beryllium (b) radial profiles on poloidally- and toroidal-oriented side surfaces. The deuterium content varies but on average it is not less than  $3 \times 10^{19} \text{cm}^{-2}$ . The analysis of side surfaces was carried out only for the two tiles. However, an inspection of the whole poloidal set of tiles (see also Fig.2(a)) have shown significant deposition on shaded sides of two inner and three outer tiles of the divertor floor

corresponding to the half of the entire set. Also the tile-supporting rails were coated in that region of the divertor. Taking into account the total area of shaded side surfaces on these tiles,  $\sim 5.3\text{m}^2$ , the assessed fuel inventory is about  $15.9 \times 10^{23}$  D atoms, i.e. nearly two times greater than found on the plasma facing surfaces. This value should again be treated as a result of a conservative approach, because the analysis depth was limited to several microns, whereas regions with thick flaking co-deposits were detected. The flake formation indicates the film thickness of at least of 25 – 40  $\mu\text{m}$ . Secondly, the results presented here give only a comparison for the divertor floor, whereas pronounced deposition was also observed on the inner vertical tiles [21].

Detailed analysis of side surfaces of Mk-IIA and GB components has not been accomplished yet (especially for Mk-IIIGB), but readily available results form a fairly consistent picture. Massive deposition of beryllium-free hydrogenated carbon films takes place in the corner of the inner leg [9,12,13]. This applies also to side surfaces of tiles located in the remote region shaded from the direct plasma impact. On the other hand, in gaps separating the other tiles only relatively thin deposits are formed as could be judged by visual inspection. In quantitative terms, the total fuel accumulation in gaps of the water-cooled Mk-I (pumping direction) may be comparable to that on remotely located water-cooled louvers and shadowed parts of tiles in the inner corner of Mk-IIA and Gas Box. However, one may suppose that there are certain differences in a scenario of material transport to remote regions of the inner divertor and to the castellated-like structure of Mk-I. This is inferred from the presence of significant beryllium content in the gaps (Be profiles in Fig.5) whilst no beryllium is observed in the shadowed region of the Mk-II divertors. Beryllium arrives to the JET divertor as species eroded from the main chamber wall (which is regularly coated by evaporation). Be migration is initiated by physical sputtering and, therefore, under cold plasma conditions ( $T_e < 4\text{-}5\text{eV}$ , i.e. below threshold energy for sputtering) its erosion and further migration is terminated [9,13]. On the contrary, carbon undergoes both physical and chemical erosion and, in the form of various hydrocarbons, can travel long distances until it becomes deposited. For that reason massive deposition of beryllium-free carbon films could occur on cold surfaces in the shadowed region of the inner divertor. When the gaps are considered, beryllium and all other elements cannot be deposited there directly from the plasma (see geometrical details in Fig.1 and 3). Therefore, they must originate from the erosion of CFC tiles and erosion of material re-deposited on them. While hydrocarbon molecules formed in this process can easily be transported towards the bottom of the divertor, sputtered beryllium and inconel components (also present in the deposit) are not volatile and can reach side surfaces only as atoms. Having in mind the tile geometry and the gap width, some atoms re-eroded from edges can certainly be deposited on a side surface of the adjacent tile. As a result very steep radial concentration profiles should be produced. This is exactly the case for the poloidally-oriented shaded surface where Be is found only close to the top of the tile. On the toroidally-oriented part (non-shaded), the greatest Be content in the gap is again found near the plasma facing surfaces, but then the profile flattens and a constant level ( $3 \times 10^{17} \text{ cm}^{-2}$ ) is detected. In this case the Be transport mechanism can not be decidedly stated, though it might be attributed to



two effects: sputtering from non-shaded edges of the adjacent tile (see Fig.3) or a parasitic glow plasma between the tiles. The latter process would offer a reasonable explanation for the migration and fairly uniform distribution of species down the divertor. Such a parasitic discharge has been observed in the pumping duct of ASDEX-Upgrade [22,23], but it should be experimentally verified, whether this phenomenon could be responsible for the deposition pattern inside gaps in the divertor. One possibility is to install a set of electrical probes facing a gap space.

The recent measurements of deuterium on MK-I tiles were performed nearly eight years after the first investigation. From the comparison of D contents in both cases one infers that there was no significant change and the fuel inventory still remains very high. This issue will be discussed in another paper.

### 3.2 TEXTOR

Analysis of ALT II tiles after campaigns lasting 14 000 – 15 000s have shown distinct separation of erosion and deposition zones. The latter ones are fairly uniformly coated with 40 – 45 $\mu\text{m}$  thick films, i.e. the growth rate is 2.5 – 3.1 $\text{nm s}^{-1}$  (total D inventory  $2.2 \times 10^{23}$ ) [19,24]. Formation of films in the gaps between tiles occurs only in the part corresponding to the extent of the deposition zone on the plasma facing surface. Taking into account that the gap depth (10-14mm) and assuming the same areal D concentration as measured on plasma facing side, one infers that the amount of material transported and retained on side surfaces in all the gaps would reach at most  $0.6 \times 10^{23}$  D atoms. This is about four times less than accumulated on top surfaces. Twice lower content ( $0.3 \times 10^{23}$ ) is derived when comparing quantities of thermally desorbed deuterium with that assessed for top surfaces by means of ion beam analysis combined with microscopy studies. The results lead to two quite contradictory conclusions regarding the inventory in gaps: (i) it is insignificant in the total balance; (ii) it might become significant if the gap depth is greater and uniform deposition continues down the slot. However, little deposition found on the inconel plate supporting the tiles might indicate that the first option should prevail.

Massive material accumulation (up to 1mm) - though containing small amount of deuterium (< 0.5 at %) – occurred on scoops and neutraliser plates, i.e. at the entrance to the pumping ducts beneath the limiter structure [19,25]. These components were studied after about 90 000s of operation and from that the film growth rate is assessed to be 11nm/s [19]. In addition, fairly thin (below 1 $\mu\text{m}$ ) but highly deuterated films (D/C ~ 0.7) were found in pumping ducts [26].

Figure 6 shows a damaged tungsten-coated graphite limiter after its exposure to power loads of 20  $\text{MW m}^{-2}$  in TEXTOR [20]. A part of the coating was also melted. Pronounced material mixing of carbon, boron and tungsten found on the top surface resulted, however, in a small inventory not exceeding  $2 \times 10^{17}$   $\text{D cm}^{-2}$  [10] measured only in areas with high content of co-deposited carbon, over  $3 \times 10^{18}$   $\text{D cm}^{-2}$ . Rutherford backscattering spectra shown in Fig.7 reflect the change of composition in radial direction along the side surface (W deposition was similar on both sides of the limiter). The surface layer at a small radial distance from the plasma consists of a fully mixed

thick carbon and tungsten layer. Massive amount of tungsten at this location is most probably related to prompt re-deposition [27] of species sputtered from the top and then mixed with an incoming flux of other impurities. The amount of tungsten in radial direction decreases but even near the limiter base (62 mm from the edge) still thick overlayer is detected,  $>1 \times 10^{17} \text{ cm}^{-2}$ . Migration of W downwards to that distant location may probably be attributed to several simultaneous processes such as (i) long-distance migration of sputtered neutrals and (ii) re-deposition of eroded and then globally transported species. A multi-step transport involving re-erosion and prompt re-deposition of species once deposited in the gap should rather be excluded, unless there is an auxiliary glow plasma formed between the tiles. This hypothesis is still to be experimentally validated. However, taking into account very significant amount of W found in the gap, the most probable reason for the observed W-deposition pattern is the transport of metal atoms evaporated from the coating subjected to high power loads. Fuel inventory not exceeding  $1.4 \times 10^{17} \text{ cm}^{-2}$  was determined on that side surface [10]. Similarly low content was measured on surfaces in the gap between graphite and tungsten blocks of the twin limiters [8].

From the very detailed analyses of permanent and test components from various locations at TEXTOR one obtains quite complex overall pattern of deposition and fuel retention. However, it seems to be clear that - due to high base temperature of PFC - the deposition in gaps and remote areas of this machine does not lead to threatening fuel inventories.

## CONCLUSIONS AND RECOMMENDATIONS

The results gathered for several limiter and divertor structures from JET and TEXTOR show that the deposition in gaps separating tiles of PFC is an issue that deserves further detailed studies. As could be expected, low temperature of water-cooled components certainly contributes to the deposition and high fuel inventory also on side surfaces. In other instances, e.g. gaps between the TEXTOR limiter tiles or between the JET tiles in the private region of Mk-I and Mk-II, the magnitude of deposition is not so meaningful.

Exact inventory levels can not be given with a higher degree of confidence, but even this estimate shows the scale of the deposition effects in gaps. The results indicate that in case of water-cooled castellated structures with sharp edges pronounced accumulation of mixed material could be expected in grooves and gaps separating the tiles. It is not our intention to give here a quantitative prediction for ITER because the data base is still too small. Secondly, the distribution of plasma facing materials (Be, W and CFC) and plasma density in the ITER divertor will be different than in any present-day device. Results shown in this paper lead to a conclusion that this not just the existence of gaps, slots or grooves on PFC that is decisive for the deposition but the arrangement and shaping of tiles with respect to the field lines. Mk-I is a good example supporting this tentative statement. However, it becomes obvious that currently developed or proposed methods of tritium removal should be tested on castellated structures in order to ensure effective fuel removal on a reasonable time scale. In turn, this calls for testing and exposures of castellated components in existing tokamaks. A test of the

macro-brush tungsten limiter at TEXTOR is the first step [4], but similar experiments should be done for CFC tiles with the ITER-like structure. Tracer techniques with rare isotopes (e.g.  $^{13}\text{C}$  [25,28- 30]) and marker tiles [25,31] would help the determination of transport mechanism to the gaps.

Instrumented tiles with electrical probes mounted in the gaps should be used to resolve the issue whether the formation of parasitic glow plasma takes place and enhances the material transport. Last but not least, side surfaces of PFC from previous experimental campaigns in different machines can be studied in more detail. This also applies to CFC vertical tiles and the entire poloidal set of castellated beryllium tiles from the Mk-I divertor.

## ACKNOWLEDGEMENTS

We are very grateful to Mr. G. Kaveney and Mr. M. Woolard for help in the inspection of JET tile in the Beryllium Handling Facility at Culham Science Centre. This work was partly supported by the NFR Contract F5102-20006021/2000.

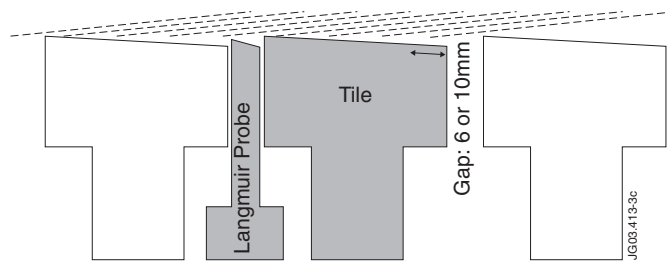
## REFERENCES

- [1]. Davis, J.W., Barabash, V., Makhankov, A., Plöchl, L. and Slattery K.T., *J. Nucl. Mater.* **258-263**, 308 (1998).
- [2]. Merola, M. et al., *Phys. Scr.* **T91**, 104 (2001).
- [3]. Daenner, W. et al., *Fusion Eng. Des.* **61-62**, 61 (2002).
- [4]. Hirai, T. et al. *J. Nucl. Mater.* **313-316**, 69 (2003).
- [5]. Coad, J.P., Rubel, M. and Wu, C.H., *J. Nucl. Mater.* **241-243**, 408 (1997).
- [6]. Coad, J.P., Andrew, P.L. and Peacock, A.T., *Phys. Scr.* **T81**, 7 (1999).
- [7]. Wienhold P. et al., *Phys. Scr.* **T94**, 141 (2001).
- [8]. Rubel, M. et al., *J. Nucl. Mater.* **283-287**, 1089 (2000).
- [9]. Coad, J.P. et al., *J. Nucl. Mater.* **290-293**, 224 (2001).
- [10]. Rubel, M., Philipps, V., Pospieszczyk, A., Tanabe, T. and Kötterl, S., *J. Nucl. Mater.* **307-311**, 111 (2002).
- [11]. Andrew, P.L. et al., *Fusion Eng. Des.* **47**, 233 (1999).
- [12]. Penzhorn, R.D. et al., *J. Nucl. Mater.* **288**, 170 (2001).
- [13]. Rubel, M. et al., *J. Nucl. Mater.* **313-316**, 323 (2003).
- [14]. Counsell, G.F and Wu, C.H., *Phys. Scr.* **T91**, 70 (2001).
- [15]. Skinner, C.H. et al., *Phys. Scr.* **T103**, 34 (2003).
- [16]. Skinner, C.H. et al., *J. Nucl. Mater.* **313-316**, 496 (2003).
- [17]. Samm, U. et al., *J. Nucl. Mater.* **162-164**, 24 (1989).
- [18]. Mayer, M. et al., *J. Nucl. Mater.* **290-293**, 381 (2001).
- [19]. Rubel, M. et al., *Phys. Scr.* **T103**, 20 (2003).
- [20]. Pospieszczyk, A. et al., *J. Nucl. Mater.* **290-293**, 947 (2001).
- [21]. Whyte, D.G., Coad, J.P., Franzen, P. and Maier, H., *Nucl. Fusion* **39**, 1025 (1999)

- [22]. Rohde, V. and Mayer, M., J. Nucl. Mater. **313-316**, 337 (2003).
- [23]. Rohde, V. and Mayer, M., Phys. Scr. **T103**, 25 (2003).
- [24]. Rubel, M., Wienhold, P. and Hildebrandt, D., J. Nucl. Mater. **290-293**, 473 (2001).
- [25]. Wienhold, P. et al., J. Nucl. Mater. **313-316**, 313 (2003).
- [26]. von Seggern, J., Wienhold, P., Hirai, T., Philipps, V. and Esser, H.G., J. Nucl. Mater. **313-316**, 439 (2003).
- [27]. Naujoks, D. and Behrisch, R., J. Nucl. Mater. **220-222**, 227 (1995)
- [28]. Wienhold, P. et al., J. Nucl. Mater. **290-293**, 362 (2001).
- [29]. Rubel, M., Wienhold, P. and Hildebrandt, D., Vacuum **70**, 423 (2003).
- [30]. Likonen, J. et al., Fusion Eng. Des., Studies of impurity deposition and implantation in JET divertor tiles using SIMS and ion beam techniques, in press.
- [31]. Coad, J.P. et al., J. Nucl. Mater. **313-316**, 419 (2003).



JG03.413-4c



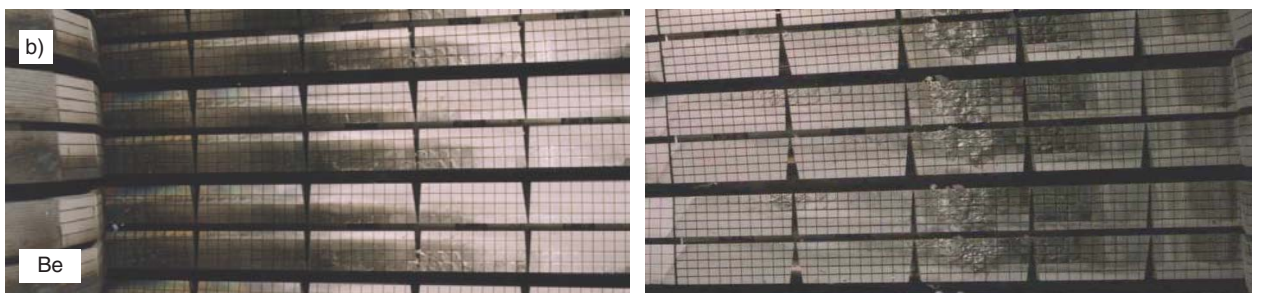
JG03.413-3c

Figure 1: JET with the Mk-I beryllium divertor (a) and schematic view showing the location of tiles and Langmuir probes (b).



a)

CFC



b)

Be

JG03.413-5c

Figure 2: Mk-I divertor tiles after operation: CFC (a) and beryllium (b)

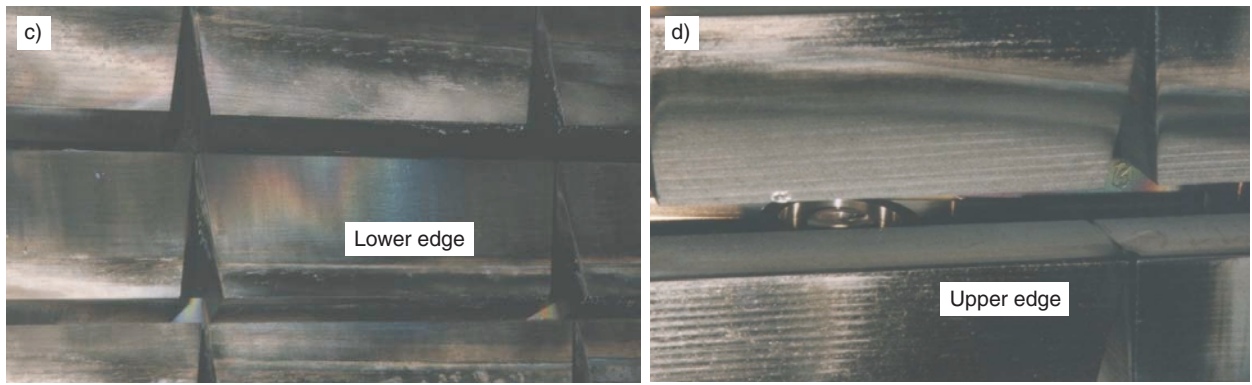


Figure 3: CFC tiles of the Mk-I divertor: top surfaces and shaded side surface (a), top surfaces and side surfaces of the shadowing tile.

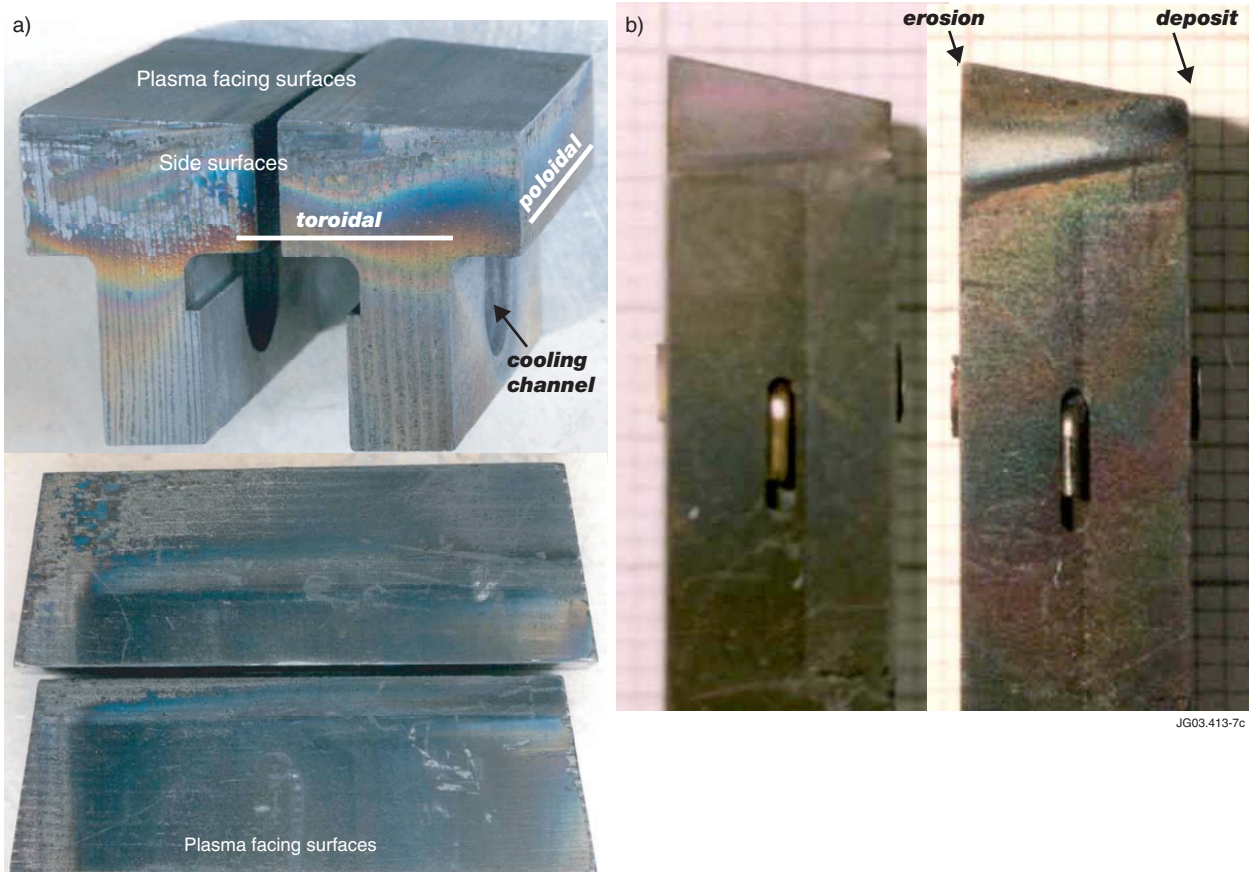


Figure 4: Exposed CFC tiles (a) and Langmuir probes (b) from the JET Mk-I divertor.

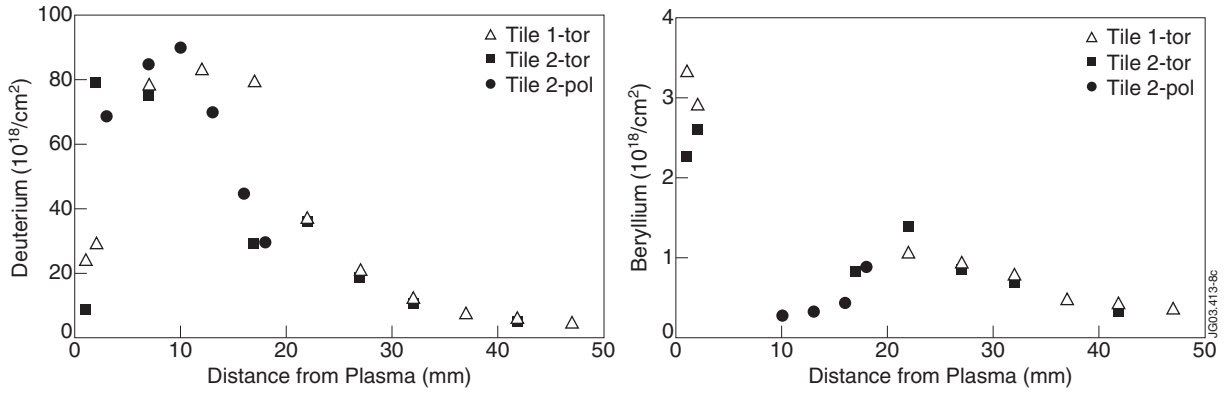


Figure 5: Distribution of deuterium (a) and beryllium (b) on side surfaces in gaps between the Mk-I CFC tiles.

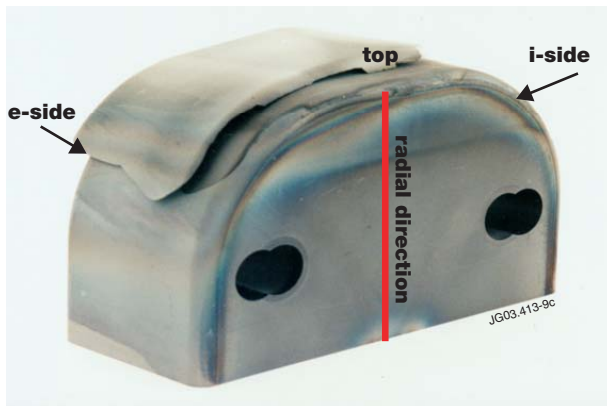


Figure 6: VPS-tungsten coated graphite poloidal limiter exposed at TEXTOR.

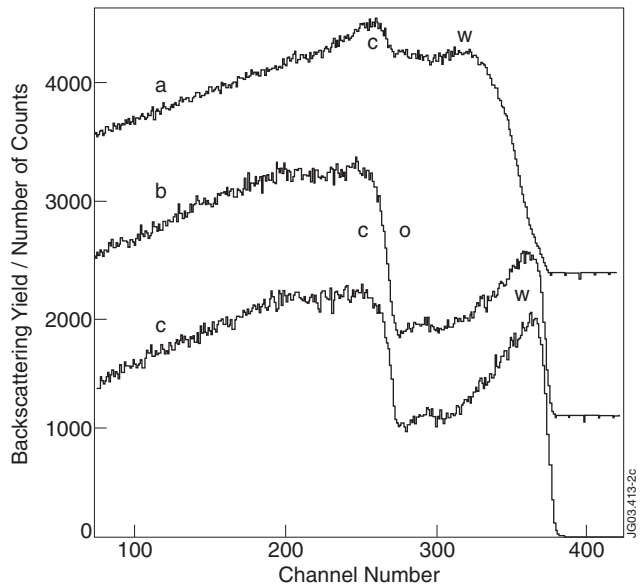


Figure 7: Carbon-tungsten mixing on the side surface of the limiter, i.e. in the gap between the limiter tiles.